HIPPOCAMPAL SURFACE DISCRIMINATION VIA INVARIANT DESCRIPTORS OF SPHERICAL CONFORMAL MAPS

Boris Gutman[1], *Yalin Wang*[1,2], *Lok Ming Lui*[1], *Tony F. Chan*[1], *Paul M. Thompson*[2]

[1] Mathematics Department, UCLA
[2] Lab. of Neuro Imaging and Brain Research Institute, UCLA School of Medicine
bgutman@ucla.edu, {ylwang,malmlui,chan}@math.ucla.edu, thompson@loni.ucla.edu

ABSTRACT

Weighted spherical harmonic shape descriptors are based on the subspaces of $L^2(\mathbb{S}^2)$ spanned by spherical harmonics of a single degree. Such shape descriptors incorporate both shape and scaling information, while preserving invariance with respect to other non-reflexive affine transformations. Thus, their application allows for direct comparison of shapes across subjects, resolutions and within-subject components. On the other hand, global conformal parametrization preserves intrinsic conformal structure and thus allows for vast differences in object scaling on the 2-sphere. As a result, surface energy is distributed more evenly across the spherical harmonic spectrum, with the higher resolution descriptors representing regions with higher conformal factor. We applied our morphometry to 96 hippocampal surfaces. The data used were 12 control and 12 Alzheimer (AD) T1 and T2 subjects. An independent-samples t-test revealed significant differences for the change in hemispheric shape difference in shape descriptors of degrees 3, 20, 22, 25 and 27, with the highest p-value of .001, t = 4.019, predicting 22 out of 24 subjects' diagnosis correctly.

1. INTRODUCTION

In brain imaging, questions of global shape patterns and hemispheric shape difference often arise. Some of the problems here are combining volume and shape differences ([1], [7]) in predictive analysis as well as finding regions of significant difference for specific diseases [8]. In our study, we present a technique of direct multiresolution registration of 3D closed surfaces in the spectral domain, which combines both scale and shape information in one measure. The data were obtained from 12 control and 12 AD 3D T1 and T2 weighted SPGR (spoiled gradient) MRI images. The images were then segmented via a topologically constrained mean curvature flow algorithm based on [2] and triangulation meshes were constructed. The meshes were mapped onto the 2-sphere according to [5] and regularly sampled. A fast spherical harmonic transform algorithm of the inverse conformal maps [6] was obtained, and finally spherical harmonic shape descriptors were computed and weighted for cross-resolution comparison. Our shape descriptors are shown to be invariant under rotation and translation in the paramter space. Also, since the conformal map completely preserves rotations in object space, the resulting shape descriptors are theoretically invariant to all rotations and translations in object space. This invariance is shown to hold in practice up to negligible discretization error. Thus, weighted spherical harmonic shape descriptors make for direct surface registration both across objects and resolutions.

This work was funded by the National Institutes of Health through the NIH Roadmap for Medical Research, Grant U54 RR021813 entitled Center for Computational Biology (CCB). The work was performed while the fourth author was on leave at the National Science Foundation as Assistant Director of the Directorate for Mathematics & Physical Sciences.

2. PREVIOUS WORK

Surface registration and comparison remain some of the most interesting problems in medical imaging. Many "classical" methods, such as first-order spherical harmonic ellipsoid alignment [3] and quarternion-based alignment methods [7] provide a coarse framework for pointwise registration. In applications of these methods, the obvious means to compare surfaces is by computing displacement at each point. The accuracy of such comparison depends on the quality of registration and the degree of surface noise. An alternative morphometry utilizes spectral representation of surface. The possibility of making such representation invariant to rotation and translation makes registration quality a non-issue for statistical analysis. Further, noisy data is usually not a problem in spectral methods, since only higher order frequencies are assumed to be affected by noise.

Gerig [3] and Shen [7] have used the first order ellipsoid method in their anatomical surface studies. After the initial first order ellipsoid prealignment, Shen used a quarternion-based method to locally minimize the distance at each regularly sampled point. Further, he used both hemispheres as one shape configuration, making cross-hemispheric differences relevant in the pointwise registration. Promising discrimination results were achieved with this method. The drawback of this method lies in that only the space of rotations and translations was considered for the final registration. Further, the first ellipsoid may not always give correct prealignment, especially if two or more of the axes have the same length.

Other methods have used a more generalized space of tranformations. In a recent work, Csernansky [1] used large diffeomorphic (differentiably bijective with differentiable inverse) mapping following Miller [4] to register hippocampal surfaces in a preclinical Alzheimer study. Here, a template is chosen at random to which the data surfaces are mapped. The average inverse mapping is then computed and its image of the template serves as the reference shape average, or the new template. Although a powerful mathematical technique it is template-dependent and thus registration results may vary with varying templates. Further, such a technique assumes a reasonable spatial pre-alignment. By contrast, spherical harmonic shape descriptors assume no pre-alignment and are completely intrinsic to the original surface.

Of course, one major drawback of our method in comparison with those above is its maladaptedness to detecting specific regional variation. In the concluding section we mention some possible statistical and analytic solutions to this problem.

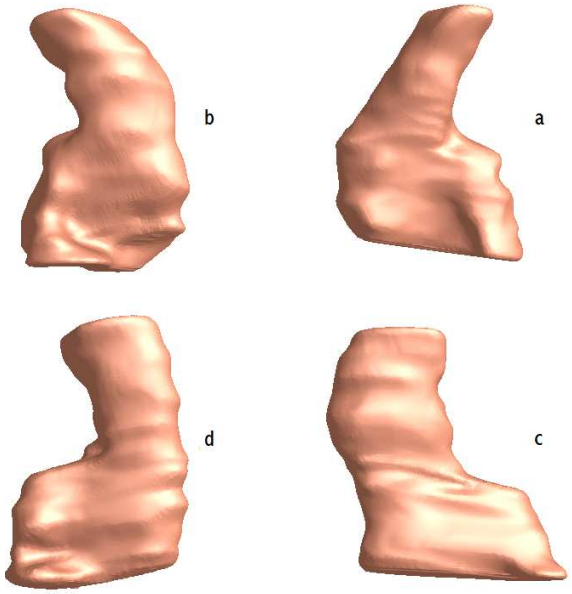

Fig. 1. Two subjects: (a) and (b) are right and left hippocampal surfaces of a male AD subject and (c) and (d) are that of a control subject

3. SPHERICAL CONFORMAL PARAMETRIZATION

In this section we give the idea behind the conformal mapping algorithm following X. Gu, Y. Wang, et al. [5]. The idea is to first find a homeomorphism $\overrightarrow{f} : M \rightarrow \mathbb{S}^2$ and then optimize it by minimizing harmonic energy. Here M is the manifold represented by a triangulation mesh of the object surface embedded in $\mathbb{R}^3$. The mesh is defined by (K, g) where K is a simplicial complex and $g : |K| \rightarrow \mathbb{R}^3$ is a function mapping the vertices of K to $\mathbb{R}^3$. For simplicity, consider a scalar piecewise-linear continuous function $f : M \rightarrow \mathbb{R}$. Let $u, v \in K$ be vertices, $\{u, v\} \in K$ the edge formed by u, v. Define the inner product on the space of PL functions by

$$< f, g >= \frac{1}{2} \sum_{\{u,v\} \in K} k_{u,v}(f(u) - f(v))(g(u) - g(v))$$

where $k_{u,v}$ is string energy. By choosing the correct string energy constants, harmonic energy is defined by

$$E(f) =< f, f >= \sum_{\{u,v\} \in K} k_{u,v}||f(u) - f(v)||^2$$

Vector functions on M to are defined by $\overrightarrow{f} = (f_1, f_2, f_3)$ Vector harmonic energy is

$$E(\overrightarrow{f}) = \sum_{i=1}^{3} E(f_i)$$

Minimizing the harmonic energy ensures that the map is harmonic i.e. that the laplacian is equal to zero. That the map is harmonic guarantees its conformality. Here, the initial homeomorphism used is the Gauss map defined by $\overrightarrow{f}(v) = \overrightarrow{n}(v), v \in M$. For details on the algorithm minimizing harmonic energy and additional constraints placed on the function to ensure convergence as well as an explanation in a more general setting, see [5].

4. SPHERICAL HARMONICS

A function $f : \mathbb{S}^2 \rightarrow \mathbb{C}$ is a spherical harmonic if it is the eigenfunction of the Laplacian operator $\Delta f = \lambda f$ where λ is a scalar multiplier. A countable set of spherical harmonics provides an orthonormal basis for the space of square-integrable functions on the sphere $L^2(\mathbb{S}^2)$. If we parameterize the sphere with a latitudinal coordinate θ and a colatitudinal coordinate ϕ, spherical harmonics are expressed explicitly:

$$Y_l^m(\theta, \phi) = \sqrt{\frac{(2l+1)(l-m)!}{4(l+m)!}} P_l^m(cos\theta) e^{im\phi}$$

for degree and order $m, l \in \mathbb{Z}$, $|m| \leq l$, where $P_l^m(x)$ is the associated Legendre polynomial.

Let f be in $L^2(\mathbb{S}^2)$. For a given order l and degree m, a spherical harmonic coefficient is defined by $\widehat{f}(l, m) =< f, Y_l^m >$, where $< f, g >$ is the usual L^2 inner product in spherical coordinates. The spherical harmonic expansion is the series

$$f(\theta, \phi) = \sum_{l=0}^{\infty} \sum_{m=-l}^{l} \widehat{f}(l, m) Y_l^m(\theta, \phi)$$

The set of all coefficients $\widehat{f}(l, m)$ is called the discrete spherical harmonic transform of f. In practice, the transform is computed with a fast algorithm described in [6], which relies on regular mesh sampling. The transform is only computed up to a certain degree $l < B$, where the B is the bandwidth.

5. SPHERICAL HARMONIC DESCRIPTORS

Let $\overrightarrow{c} : \mathbb{S}^2 \rightarrow \mathbb{R}^3$ represent a surface conformal parametriztion. We regularly sample the discrete map on the sphere using a matching area algorithm and linear interpolation. Next, we compute the spherical harmonic transform of each component scalar map. The result is a set of vector spherical harmonic coefficients in $\mathbb{C}^3$

$$\{\widehat{\overrightarrow{c}}(l, m)\} = \{[\widehat{c}_1(l, m), \widehat{c}_2(l, m), \widehat{c}_3(l, m)]^T : |m| \leq l \leq B\}$$

where B is the bandwidth. Next, we obtain the unweighted spherical harmonic descriptors:

$$s(l) = \sum_{i=1}^{3} \sum_{m=-l}^{l} ||\widehat{c}_i(l, m)||^2$$

Invariance of these descriptors is shown as follows. First, the norm of a function in $L^2(\mathbb{S}^2)$ does not change with rotation. Second, for a spherical function $p_l \in Span\{Y_l^{-l}, Y_l^{-l+1}, ..., Y_l^l\}$, and an element of the rotation group $g \in SO(3)$ and its associated operator $\Lambda(g)$, the transformed function remains in the same subspace of $L^2(\mathbb{S}^2) : \Lambda(g)(p_l) \in Span\{Y_l^{-l}, Y_l^{-l+1}, ..., Y_l^l\}$. Thus,

$$\sum_{m=-l}^{l} |\widehat{p_l}(l, m)|^2 = ||p_l||_2^2 = ||\Lambda(g)(p_l)||_2^2 = \sum_{m=-l}^{l} |\widehat{\Lambda(g)(p_l)}(l, m)|^2$$

Further, the linearity of $\Lambda(g)$ implies $f(\theta, \phi) = \sum_{l=0}^{B-1} p_l \Rightarrow \Lambda(g)[f(\theta, \phi)] = \sum_{l=0}^{B-1} \Lambda(g)(p_l)$. From this it is clear that our descriptors are invariant as each scalar component norm must remain invariant within each subspace. Translational invariance is achieved

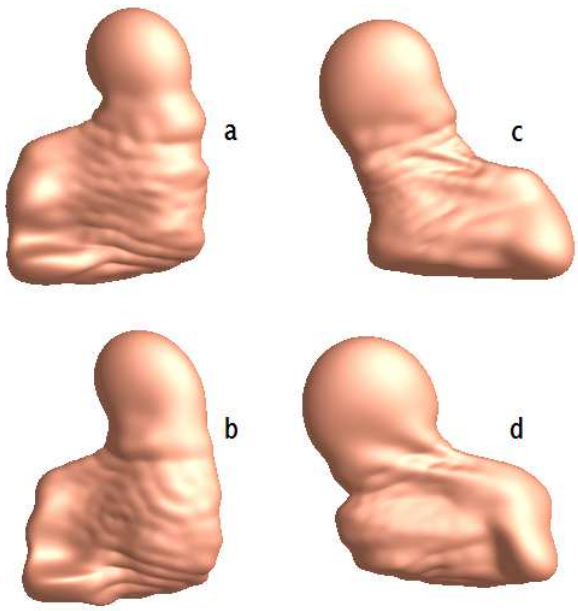

Fig. 2. T1 and T2 reconstructions from frequencies 20,22,25,27 of the control subject from figure 1: (a) T1 left hippocampus (b) T2 left hippocampus (c) T1 right hippocampus (d) T2 right hippocampus

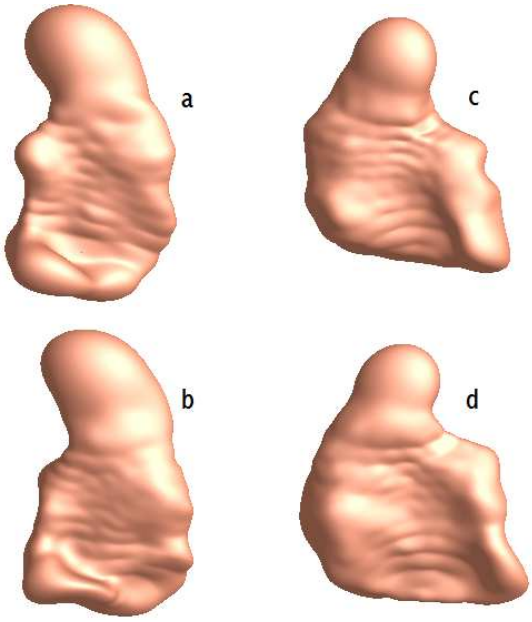

Fig. 3. T1 and T2 reconstructions from frequencies 20,22,25,27 of the AD subject from figure 1: (a) T1 left hippocampus (b) T2 left hippocampus (c) T1 right hippocampus (d) T2 right hippocampus

trivially by ignoring the zeroth coefficient, which is alone responsible for translation. Thus, we produce a quasi-unique multi-resolution global shape representation. Now, surface comparison is possible directly at each resolution level.

To enable meaningful cross-resolution comparison, we randomly select a subgroup of N subjects and compute normalization constants for each degree:

$$C(l) = \frac{1}{N} \sum_{i=1}^{N} \sum_{k=1}^{B-1} s_i(k)/s_i(l)$$

Our final weighted shape descriptors are defined as $n(l) = s(l)C(l)$. Such descriptors allow for measure of relative resolution difference within and between surfaces while incorporating scaling information. These may be especially useful for large-population studies of global shape change. Because the conformal map preserves the intrinsic conformal structure of a surface, regional differences may be estimated heuristically. Variation in regions of higher conformal factor corresponds to variation in higher degree shape descriptors.

6. EXPERIMENTAL RESULTS

Our experimental results confirm rotational invariance up to discretization and sampling error. Relative error due to a random rotation is within 1 %.

Initially, we ran a 3-way ANOVA on T2 - T1 differences of normalized descriptors with hemisphere, diagnosis and frequency as factors. We then examined hemisphere - frequency interaction at each of the 255 frequencies. Frequencies 3, 20, 22, 25 and 27 gave the most significant interaction between diagnosis and hemisphere. Independent samples t-tests between control and AD subjects for hemispheric differences at significant degree combinations are displayed in figure 4. The most significant combination was $s(20) - s(3)/2$ (df = 22, t = 4.019, P = .001).

Next, a 3-Way ANOVA as above was ran on just the significant frequencies we mentioned. Here, we see that there is a significant three-way interaction between frequency, diagnosis and hemishpere, making cross-resolution comparison useful. The significant results are for interaction between diagnosis and hemisphere (df = 1, F = 20.957, $\alpha < .001$) and interaction between frequency, diagnosis and hemisphere (df = 4, F = 3.233, $\alpha = .013$). Here, "df" stands for "degrees of freedom," "F" is the value from the F-distribution (a continuous distribution which arises when comparing variances between two samples) based on sums of squares and "α" is the tail of the distribution at the given F-value.

From the interaction plots in figure 5, we see that the three-way interaction in the ANOVA test is due entirely to descriptor of degree 3. At this frequency, the magnitude change in AD subjects is roughly equal in both hemispheres, while in control subjects it is much greater in the right hemisphere. The exact opposite occurs at frequency 20, and a pattern similar to 20 is seen in the other significant frequencies. An explanation for this may be as follows. Change at frequency 3 is more sensitive to a change in the overall volume of the object, while change at the mid-level frequencies corresponds to change in a region with a high conformal factor. Thus, results above indicate a bilateral volume reduction for AD and a greater volume reduction in the right hemisphere for control subjects. Conversely, the reduction of the extreme conformal factor area is bilateral in control subjects and increased in the right hemisphere in AD subjects. This hypothesis remains to be confirmed through spatial registration of our surfaces and compared with other reports on AD.

7. CONCLUSION AND FUTURE WORK

Spherical harmonic shape descriptors provide a reasonable means of surface dicrimination in disease studies. Unlike other morphometric techniques, they allow cross-resolution comparison, which has been shown in this study to be significant. Further, for studies involving multiple closed surfaces per subject, such as the left and right hippocampus, cross-component comparison is just as trivial as cross-subject analysis, giving rise to a new set of data. In experiments, our global metric outperformed many localized metrics described above, giving purpose to future refinements of our method.

To further develop use of spherical harmonics as a means of shape representation, we would like to:

(1)Develop a direct registration method via spherical cross-correlation.

(2)Develop a spherical harmonic representation which is intrinsically optimal with respect to the conformal structure of the surface, thus integrating the theory of spherical harmonics with global conformal mapping.

(3)Apply within-level PCA-alignment of spherical harmonics and use coarse spatial registration for regional variation detection.

Independent Samples Test

		Levene's Test for Equality of Variances		t-test for Equality of Means						
									95% Confidence Interval of the Difference	
		F	Sig.	t	df	Sig. (2-tailed)	Mean Difference	Std. Error Difference	Lower	Upper
mean(frequency = 20, 22)	Equal variances assumed	.257	.617	3.515	22	.002	287.38919	81.75657	117.83645	456.94193
	Equal variances not assumed			3.515	20.639	.002	287.38919	81.75657	117.18606	457.59233
mean(frequency = 20, 22, 25)	Equal variances assumed	.130	.722	3.778	22	.001	263.59414	69.77424	118.89122	408.29707
	Equal variances not assumed			3.778	21.678	.001	263.59414	69.77424	118.76631	408.42198
mean(frequency = 20, 22, 25, 27)	Equal variances assumed	.094	.762	3.517	22	.002	342.43029	97.35227	140.53405	544.32654
	Equal variances not assumed			3.517	21.824	.002	342.43029	97.35227	140.43958	544.42101
frequency20	Equal variances assumed	.883	.358	3.744	22	.001	283.51096	75.72355	126.46993	440.55199
	Equal variances not assumed			3.744	20.644	.001	283.51096	75.72355	125.86949	441.15244
frequency22	Equal variances assumed	.097	.759	3.011	22	.006	291.26742	96.74389	90.63287	491.90198
	Equal variances not assumed			3.011	21.492	.007	291.26742	96.74389	90.35748	492.17737
frequency25	Equal variances assumed	.171	.683	2.675	22	.014	216.00404	80.75181	48.53503	383.47305
	Equal variances not assumed			2.675	21.851	.014	216.00404	80.75181	48.46894	383.53914
frequency27	Equal variances assumed	1.256	.274	2.279	22	.033	236.50845	103.79691	21.24683	451.77007
	Equal variances not assumed			2.279	19.965	.034	236.50845	103.79691	19.96747	453.04944
mean(frequency = 20, 25, 27)	Equal variances assumed	.405	.531	3.268	22	.004	245.34115	75.06519	89.66548	401.01683
	Equal variances not assumed			3.268	21.796	.004	245.34115	75.06519	89.58095	401.10136
frequency3	Equal variances assumed	1.632	.215	-2.115	22	.046	-100.37030	47.44943	-198.77441	-1.96620
	Equal variances not assumed			-2.115	20.633	.047	-100.37030	47.44943	-199.15374	-1.58686
frequency20 - 0.5*frequency3	Equal variances assumed	2.293	.144	4.019	22	.001	333.69612	83.02175	161.51955	505.87268
	Equal variances not assumed			4.019	17.815	.001	333.69612	83.02175	159.14403	508.24820
frequency20 - frequency3	Equal variances assumed	3.925	.060	4.007	22	.001	383.88127	95.79609	185.21235	582.55019
	Equal variances not assumed			4.007	16.184	.001	383.88127	95.79609	180.99021	586.77232

Fig. 4. T-Tests at degrees 3,20,22,25 and 27

8. REFERENCES

[1] J. G. Csernansky, L. Wang, J. Swank, J. P. Miller, M. Gado, D. McKeel, M. I. Miller, and J. C. Morris, "Preclinical detection of Alzheimer's disease: hippocampal shape and volume predict dementia onset in the elderly," Neuroimage. Vol 25 Issue 3, pp 783-792, 15 April 2005

[2] X. Han, C. Xu, J. Prince, "A Topology-Preserving Level Set Method for Geometric Deformable Models," IEEE Transactions on Pattern Analysis and Machine Intelligence, vol 25 No. 6 pp.755-769, June 2003

[3] G. Gerig, M. Styner, D. Jones, D. Weinberger, and J. Lieberman, "Shape analysis of brain ventricles using spharm," presented at the IEEE Workshop on Mathematical Methods in Biomedical Image Analysis (MMBIA'01), Kauai, HI, December 2001.

[4] M. I. Miller, "Computational anatomy: shape, growth, and atrophy comparison via diffeomorphisms" Neuroimage Vol. 23, Supp 1, pp. S19-S33, 2004.

[5] X. Gu, Y. Wang, T. F. Chan, P. M. Thompson, and S. Yau "Genus Zero Surface Conformal Mapping and Its Application to Brain Surface Mapping" IEEE Transactions on Medical Imaging, Vol. 23, No. 8, p. 949, August 2004

[6] D. Healy, D. Rockmore, P. Kostelec, and S. Moore, "Ffts for the 2-sphere-Improvements and variations," J. Fourier Anal. Applicat., vol. 9, no. 4, pp. 341-385, 2003.

[7] L. Shen, F. Makedon, and A. Saykin, "Shape-based Discriminative Analysis of Combined Bilateral Hippocampi using Multiple Object Alignment," Medical Imaging 2004, SPIE Proc. 5370, pp. 274-282, San Diego, Feb. 2004.

[8] L. Shen, A. Saykin, T. McHugh, J. West, L. Rabin, H. Wishart, M Chung, and F. Makedon, "Morphometric Analysis of 3D Surfaces: Application to Hippocampal Shape in Mild Cognitive Impairment," CVPR 2005, June 2005.

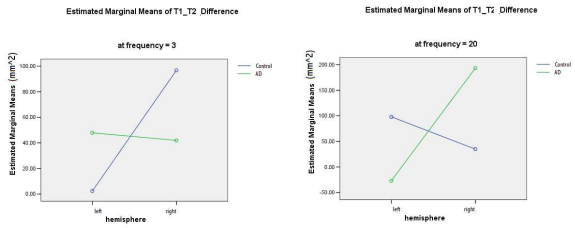

Fig. 5. hemishphere-diagnosis interactions for degree 3,20

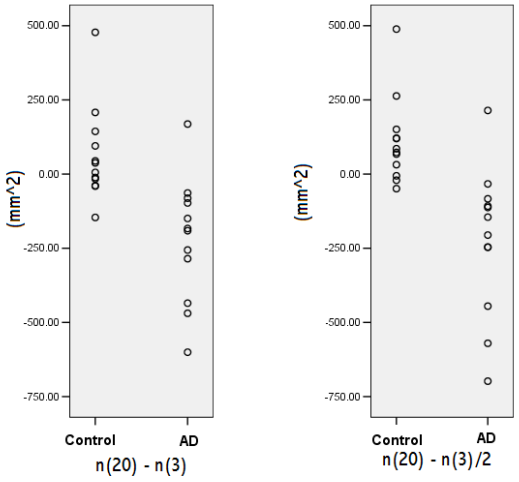

Fig. 6. Scatter plots for two selected degree combinations of change in hemishperic shape difference. There is little overlap.